SIX DAYS ■ THREE CONFERENCES ■ ONE EXHIBITION

EUROPEAN MICROWAVE WEEK 2017
NÜRNBERG CONVENTION CENTER,
NUREMBERG, GERMANY
8TH - 13TH OCTOBER 2017

EUROPEAN MICROWAVE WEEK
NÜRNBERG CONVENTION CENTER
NUREMBERG, GERMANY
8TH-13TH OCTOBER 2017
www.eumweek.com

EUROPEAN MICROWAVE WEEK 2017
CONFERENCE PROGRAMME

EUROPE'S PREMIER MICROWAVE, RF, WIRELESS AND RADAR EVENT

REGISTER ONLINE AT:
www.eumweek.com

EuMA European Microwave Association

Organised by: horizon house

Official Publication: Microwave Journal

Co-sponsored by: IEEE

Co-sponsored by: MTT-S

Supported by: IET The Institution of Engineering and Technology

Supported by: VDE ITG

EuMIC 2017
The 12th European Microwave Integrated Circuits Conference
Co-sponsored by:

47TH EUROPEAN MICROWAVE CONFERENCE 2017
The 47th European Microwave Conference
Co-sponsored by:

EuRAD 2017
The 14th European Radar Conference
Co-sponsored by:

	Hongkong	Kiew	Riga
	EuMC14 **Antennas for mm-Wave Applications** Chair: Ioan Lager, Delft University of Technology Co-Chair: Alessandro Galli, Sapienza University of Rome	**EuMC15** **Impedance Matching Solutions for GaN Power Amplifiers** Chair: Eric Kerhervé, IMS laboratory Co-Chair: Christian Fager, Chalmers University of Technology	**EuMC16** **Special Session: Novel Microwave Devices and Measurements in Central Europe** Chair: Jozef Modelski, Warsaw University of Technology Co-Chair: Jan Vrba, Czech Technical University in Prague
08:30 - 08:50	***EuMC14-1*** ***Mixed-Domain Gating Algorithm for Time-Domain Characterisation of Millimetre-Wave Antennas*** Lars Ohlsson, Iman Vakili, Daniel Sjöberg, Lars-Erik Wernersson, Lund University	***EuMC15-1*** ***Triband 1.2/1.8/2.7 GHz Doherty Power Amplifier Using Novel Output Combining Network*** Bassem Abdelrahman, Hesham Ahmed, Military Technical College	***EuMC16-1*** ***Direction-of-Arrival Estimation Using an ESPAR Antenna with Simplified Beam Steering*** Lukasz Kulas, Gdansk University of Technology
08:50 - 09:10	***EuMC14-2*** ***A Zero-IF Auto-Calibration System For Phased Array Antenna*** Mehdi Salehi, Safieddin Safavi-Naeini, University of Waterloo	***EuMC15-2*** ***Harmonics Suppressed Band-Pass Matching Network for High Efficiency Power Amplifier*** Junhyung Jeong[1], Phirun Kim[1], Yongchae Jeong[1], Jongsik Lim[2], [1]Chonbuk National University, [2]Soonchunhyang University	***EuMC16-2*** ***Microwave Amplifiers Using GaN HEMTs on Truly Bulk GaN Substrates*** Marcin Góralczyk[1], Dawid Kuchta[1], Wojciech Wojtasiak[1], Andrzej Taube[1,2], [1]Warsaw University of Technology, [2]Institute of Electron Technology
09:10 - 09:30	***EuMC14-3*** ***A Novel Synthesis Method for Millimeter-Wave Antenna with Contoured-Beam at Near-Field Region*** Gang Xu, Institute of Electronic Engineering, China Academy of Engineer Physics	***EuMC15-3*** ***A Sequential Power Amplifier at 3.5 GHz for 5G Applications*** Philipp Neininger[1,2], Christian Friesicke[1], Sebastian Krause[1], Dirk Meder[1], Roger Lozar[1], Thomas Merkle[1], Rüdiger Quay[1], Thomas Zwick[2], [1]Fraunhofer Institute for Solid State Physics IAF, [2]Karlsruhe Institute of Technology (KIT)	***EuMC16-3*** ***Tunable Shielded Dielectric Resonator Short-Circuited at the Disk Face*** Kostiantyn Savin[1], Victor Kazmirenko[1], Yuriy Prokopenko[1], Borys Pratsiuk[2], Guy Vandenbosch[3], [1]National Technical University of Ukraine «KPI», [2]Cyklum Co., [3]Katholieke Universiteit Leuven
09:30 - 09:50	***EuMC14-4*** ***Analysis of Photoconductive Antennas Power Radiation by Norton Equivalent Circuit*** Alessandro Garufo, Giorgio Carluccio, Nuria Llombart Juan, Andrea Neto, Ioan Lager, Delft University of Technology	***EuMC15-4*** ***Revisiting Power vs. Bandwidth in Broadband CW Amplifiers by Exploring 100 V Bias Operation*** Gabriele Formicone, Jeff Burger, James Custer, Richard Keshishian, Integra Technologies, Inc.	***EuMC16-4*** ***CNT-Based Microwave Filter for C and X-Band Applications*** Martino Aldrigo[1], Mircea Dragoman[1], Alina Cristina Bunea[1], Dan Neculoiu[1], Stephane Xavier[2], Afshin Ziaei[2], [1]National Institute for Research and Development in Microtechnologies - IMT, [2]TRT France
09:50 - 10:10	***EuMC14-5*** ***Investigation and Development of Custom-Designed Calibration Substrates: An Introduction*** Maren Willemsen, Sybille Holzwarth, Oliver Litschke, IMST GmbH	***EuMC15-5*** ***Highly Efficient Wideband Harmonic-Tuned Power Amplifier Using Low-Pass Matching Network*** Khondker Rabbi, Jiafeng Zhou, Yi Huang, University of Liverpool	***EuMC16-5*** ***SIW Choke-Based Technique for Accurate Dielectric Measurements in the 3.5 – 5 GHz Band*** Valentin Buiculescu, Martino Aldrigo, Alexandra Stefanescu, IMT Bucharest

Harmonics Suppressed Band-pass Matching Network for High Efficiency Power Amplifier

Junhyung Jeong, Phirun Kim, and Yongchae Jeong
Division of Electronics and Information Engineering,
Chonbuk National University
Jeonju-si, Republic of Korea
jjunh05@jbnu.ac.kr

Jongsik Lim
Department of Electrical Engineering
Soonchunhyang University
Asan-si, Repiblic of Korea

***Abstract*— In this paper, the harmonics suppressed band-pass matching network for high efficiency power amplifier (PA) that can provide operating band impedance matching as well as suppressed out-of-band signals simultaneously is proposed. The proposed harmonics suppressed band-pass matching network consists of a coupled line, a λ/2 length open stub, and a λ/6 length bias line terminated with a bypass capacitor for drain bias. For an experimental validation, the PA with the proposed output harmonics suppressed band-pass matching network was designed and fabricated at the 2.14 GHz (WCDMA band). The measurement results show that the output power and drain efficiency at saturation point are 42.7 dBm and 71.2%, respectively. Compared with reference class F^{-1} PA, the proposed PA has more sharp out-of-band suppression characteristic.**

Keywords—band-pass, harmonics suppression, high efficiency, matching network, power amplifiers;

I. INTRODUCTION

Since the start of the wireless communication service, the service providers must transmit the signal within the allocated frequency band so as not to affect the other communication system. In order to satisfy these characteristics, the band-pass filter (BPF) of the transmitter and receiver front-end has become an essential component. In the conventional communication system, the power amplifier (PA) and the BPF were independently designed with 50 Ω reference impedance and connected in series. As a result, the insertion loss of the BPF to satisfy frequency limited air-interface regulation of the communication standard increases the output power level of the PA. Therefore, the efficiency of the overall system is reduced due to the increase of the insertion loss of the BPF.

In order to overcome these problems, design techniques for PAs with band-pass characteristics have been reported. [1] presented a co-design method of BPF and PA. The designed cavity BPF satisfied the output impedance matching with low insertion loss and sharp band-pass characteristics due to the high Q factor. However, this paper did not consider harmonic characteristics to obtain high efficiency characteristics of PA. In [2], the couple-line impedance transformer was used for the impedance matching and DC-block. But, it also didn't consider harmonics termination for the high efficiency characteristics. [3] proposed the frequency band selective matching network for high efficiency PA. It considered fundamental impedance matching, harmonics suppression, and band-pass characteristics, simultaneously. However, this circuit could cover only positive reactance area of load impedance.

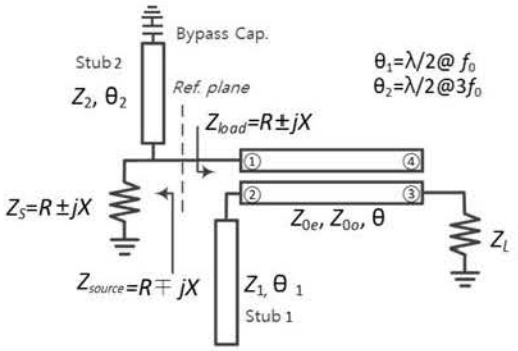

Fig. 1. Proposed harmonics suppressed band-pass matching network.

Many techniques have been introduced to obtain high efficiency characteristics of PAs [4]-[10]. One common feature of such high efficiency PAs is to match harmonic components to reactive points. Therefore, a new harmonics suppressed band-pass matching network is required to obtain impedance matching, high efficiency with harmonics suppression, and band-pass characteristics, simultaneously.

In this paper, harmonics suppressed band-pass matching network (HSBMN) for high efficiency PA is presented. The proposed HSBMN provides pass-band impedance matching, band-pass and harmonics termination characteristics with single circuit. The theoretical analysis of the proposed HSBMN and experimental results of the PA with the HSBMN are provided.

II. HARMONICS SUPPRESSED BAND-PASS MATCHING NETWORK

Fig. 1 show the structures of the proposed HSBMN. The HSBMN consists of a parallel coupled line with electrical length θ, λ/2 open stub (stub 1) at fundamental frequency (f_0) and λ/2 bias line (stub 2) at $3f_0$ terminated with a bypass capacitor. The load termination impedance Z_L is 50 Ω and Z_S is a conjugate impedance of optimum load point (Z_{opt}) of PA obtained by load-pull measurement. From the reference plane, each input impedance Z_{load} and Z_{source} at the f_0 are described as

$$Z_{source}\big|_{@f_0} = \frac{Z_S Z_2^2 3}{Z_S^2 + Z_2^2 3} + j\frac{Z_S^2 Z_2 \sqrt{3}}{Z_S^2 + Z_2^2 3}, \quad (1)$$

$$Z_{load}\big|_{@f_0} = \frac{Z_L B^2 \csc^2\theta}{Z_L^2 + A^2\cot^2\theta} + j\left(\frac{B^2\csc^2\theta A\cot\theta}{Z_L^2 + A^2\cot^2\theta} - A\cot\theta\right), \quad (2)$$

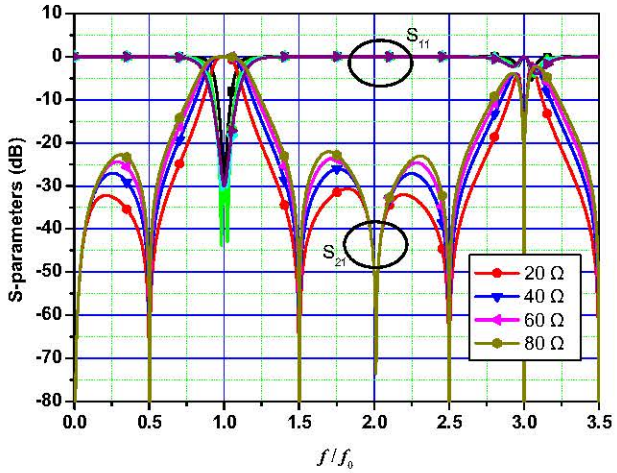

Fig. 2. *S*-parameter characteristics according to Z_1 with normalized frequency.

TABLE I. SIMULATION PARAMETERS

Z_{0o} [Ω]	Z_{0e} [Ω]	Z_1 [Ω]	Z_2 [Ω]	θ [degree]	S_{11} [dB]
60	106.06	41.3	90	89.44	-30

where Z_2 is characteristic impedance of bias line. A and B in Eqs. (1) and (2) are expressed as

$$A=\frac{Z_{0e}+Z_{0o}}{2}, \quad (3a) \qquad B=\frac{Z_{0e}-Z_{0o}}{2}, \quad (3b)$$

where Z_{0e} and Z_{0o} are even and odd impedances of coupled line, respectively. For the matching condition at f_0, Z_{source} and Z_{load} must be a conjugate impedance relation. Therefore, when the Z_2, Z_{0o}, and return loss (S_{11}) are selected by designer, Z_{0e} and Z_1 can be obtained as follows.

$$Z_{0e}=Z_{0o}+2Z_S\sqrt{\frac{r\left(1+S_{11}\big|_{f=f_0}\right)}{\left(1-S_{11}\big|_{f=f_0}\right)}} \quad (4)$$

$$Z_1=\frac{x}{r-1}=\frac{Z_{0e}+Z_{0o}}{r-1}, \quad (5)$$

where r and S_{11} are impedance transforming ratio of Z_L and Z_{opt} (Z_L/Z_{opt}) and the predefined return loss value, respectively. Finally, θ of the coupled line can be obtained by solving Eq. (6).

$$\cot^3\theta+a\cot^2\theta+b\cot\theta+c=0, \quad (6)$$

where

$$a=-\frac{AX'}{\left(A^2-B^2\right)} \quad (7a), \qquad b=\frac{\left(Z_L^2-B^2\right)}{\left(A^2-B^2\right)} \quad (7b),$$

$$c=-\frac{X'Z_L^2}{A\left(A^2-B^2\right)} \quad (7c), \qquad X'=\frac{Z_S{}^2Z_2\sqrt{3}}{Z_S{}^2+Z_2^2 3}. \quad (7d)$$

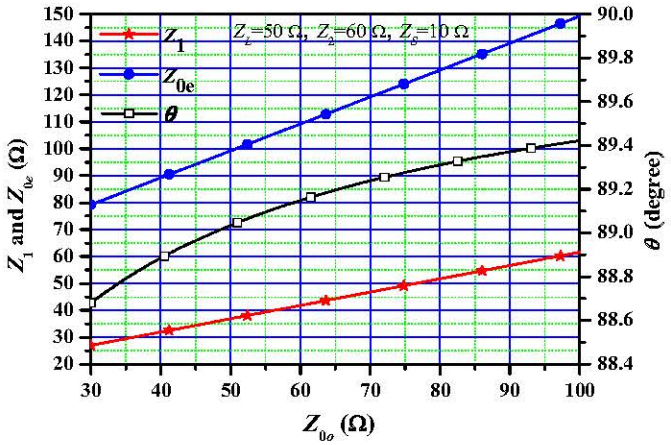

Fig. 3. Tendencies of Z_1, Z_{0e}, and θ accroding to Z_{0o}.

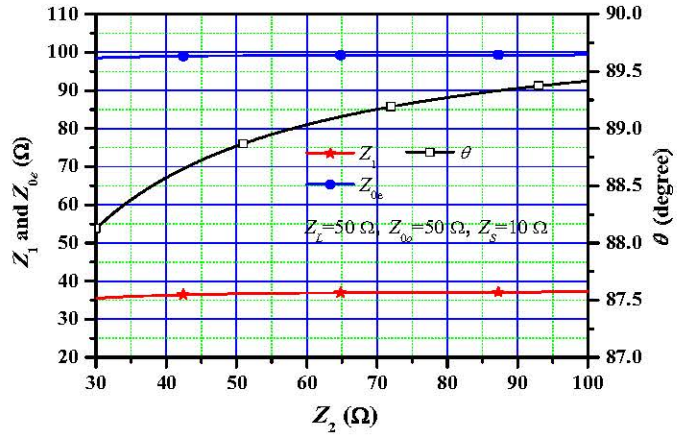

Fig. 4. Tendencies of Z_1, Z_{0e}, and θ accroding to Z_2.

Fig. 2 shows the simulated *S*-parameters according to Z_1 with the normalized frequency (f_0 = 2.14 GHz). Used parameters in simulation are listed in Table 1. The passband bandwidth and frequency selectivity characteristics are changed to narrower and sharper while maintaining a 30 dB return loss magnitude at the f_0, and the minimum out-of-band suppression characteristic is also improved as Z_1 decreases. Therefore, the proposed HSBMN can control pass-band bandwidth and frequency selectivity characteristics. In addition, the $2f_0$ and $3f_0$ harmonic suppression characteristics are well maintained.

To help design procedures of HSBMN, the tendencies between design parameters are shows in the Figs. 3 and 4. Fig. 3 shows Z_1, Z_{0e}, and θ variations according to Z_{0o} in conditions of Z_L = 50 Ω, Z_2 = 60 Ω, and Z_S = 10 Ω. As Z_{0o} decreases, all parameters values are decreased. Therefore, with smaller Z_{0o}, HSBMN would be realized with smaller size, and narrower bandwidth and better frequency selective characteristics can be obtained. As shown in Fig. 4, Z_1 and Z_{0e} are not much variated but θ is reduced as Z_2 decreases.

The design parameters should be selected in the ranges of realizable values using Figs. 3 and 4 for the specific PCB. In addition, the proposed HSBMN is physically isolated between input and output ports by the coupled line. Therefore, it does not need additional DC-blocking capacitors.

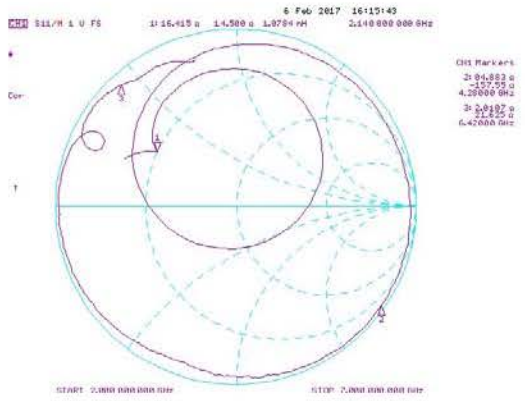

Fig. 5. Fabricated output HSBMNM measurement result.

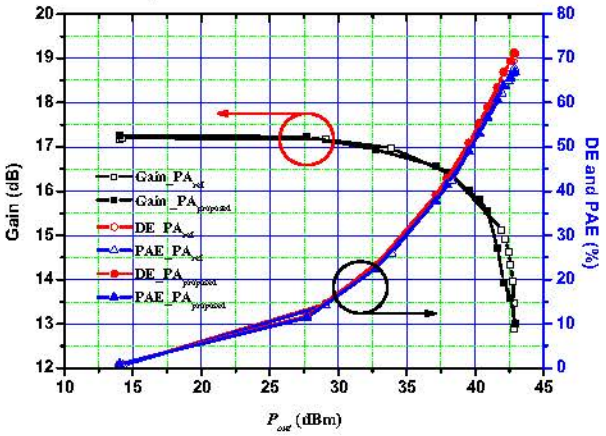

Fig. 6. Measured gain, drain effiency, power added efficiency results of the reference PA and proposed PA with HSBMN.

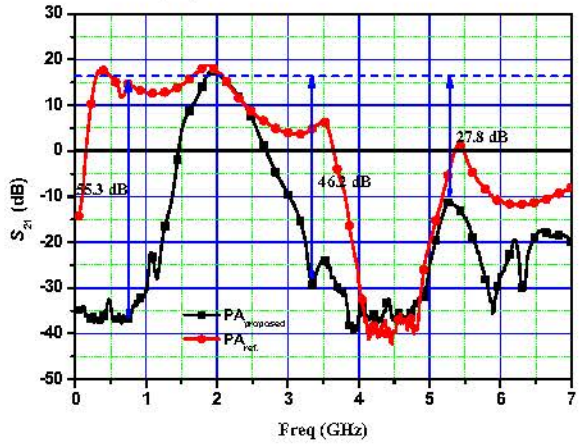

Fig. 7. S_{21} comparison between reference PA and proposed PA with HSBMN.

III. PA design with HSBMN

For an experimental validation, the PA with HSBMN was designed using a 10 W GaN HEMT transistor (CGH40010) from Wolfspeed for the WCDMA downlink band (f_0 = 2.14 GHz). The selected bias conditions were V_{DD} = 28 V, V_{GS} = -2.75 V, and I_{DQ} = 200 mA. And simulated Z_{opt} is 16.5 + j14.7 Ω with power added efficiency (PAE) of 72.8 % and saturation output power of 42.3 dBm. The input matching impedances of PA at f_0 and $2f_0$ are chosen 2.8 + j0.35 Ω and 2 + j110 Ω by source-pull simulation result.

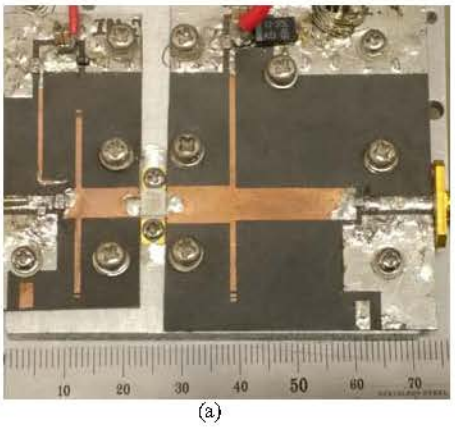

(a)

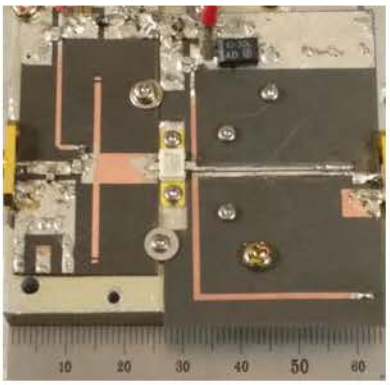

(b)

Fig. 8. Photographs of fabricated (a) reference PA and (b) proposed PA with HSBMN.

The output matching networks of the PA were realized with general transmission line matching network and the proposed HSBMN. The reference PA was designed inverse class F technique in [7] with same impedance points and transmission line output matching network for the performance comparison. The used PCB was RT/Duriod 5880 substrate from Rogers, Inc., with dielectric constant (ε_r) of 2.2 and thickness (h) of 31 mils.

Fig. 5 show the measured input impedance of the proposed HSBMN looking from Z_S in Fig. 1. The input impedance of the proposed HSBMN is well matched with the optimum load impedance. Moreover, the impedances at $2f_0$ and $3f_0$ are quasi-open-circuited and quasi-short-circuited, respectively, which can provide high efficiency characteristics in the PA design.

Fig. 6 shows the measured gains drain efficiency (DE) and PAE performances of two PAs at f_0 according to the output powers. The measurement results show that the output power, DE and PAE of the PA with HSBMN are 42.5 dBm, 71.3%, and 68.7%, respectively, at the saturation point. The output power, DE, and PAE of reference PA are 42.3 dBm, 72.2%, and 69%, respectively. As shown in the results, it can be seen that the proposed HSBMN has similar efficiency and output power characteristics compared with the conventional high efficiency power amplifier.

The measured return loss and small signal gain of both PAs are around 10.92 dB and 17.26 dB at f_0. Fig. 7 shows comparison of the measured small-signal gain responses of both PAs. The signal attenuations of PA with HSBMN at $2f_0$

and $3f_0$ are 35.7 dB and 30.12 dB, respectively. The difference between f_0 and out-of-band gains is more than 27.8 dB. In addition, the 55.3 dB and 46.2 dB differences between the f_0 and the out-of-band gains are obtained at around $0.5f_0$ (1.07 GHz) and $1.5f_0$ (3.21 GHz), respectively. Therefore, it prove that the proposed HSBMN can provide similar efficiency and output power characteristics as the conventional high efficiency power amplifier and good harmonics suppressed band-pass characteristics.

Fig. 8 shows photographs of the fabricated both PAs. Each circuit size are 75 × 50 mm^2 (reference PA) and 63 × 55 mm^2 (PA with HSBMN). The circuit size of PA with HSBMN can be minimized by bending of shunt open stub (stub 1).

IV. CONCLUSION

In this paper, the harmonics suppressed band-pass matching network for high efficiency power amplifier is described. The power amplifier with the harmonics suppressed band-pass matching network provides selective pass-band and out-of-band suppression characteristics while high efficiency and output power characteristic are maintained due to the 2nd and 3rd harmonics suppression, simultaneously. If the proposed circuits are used not only in the output matching network but also in the input matching network, the harmonics suppressed band-pass characteristics can be enhanced. The designed power amplifier also can reduce the burden of the RF transmitting band pass filter. As a results, overall system efficiency will be improved.

ACKNOWLEDGMENT

Research reported in this work has been supported by ICMTC (Institute of Civil-Military Technology Cooperation) of Korea under an ICMTC program (16-CM-SS-16).

REFERENCES

[1] K. Chen, J. Lee, W. J. Chappell, and D. Peroulis, "Co-design of highly efficiency power amplifier and high-Q output bandpass filter," *IEEE Trans. Microw. Theory Tech.*, vol. 61, no. 11, pp. 3940-3950, Dec. 2013.

[2] Y. Wu, Y. Liu, S. Li, and S. Li, " A novel high-power amplifier using a generalized coupled-line transformer with inherent DC-block Function," *Progress in Electromagnetics Research*, vol. 119, pp. 171-190, Jul. 2011.

[3] J. Jeong, P. Kim, and Y. Jeong, "High efficiency power amplifier with frequency band selective matching network," *Microwave and Optical Technology Letters*, vol. 57, no. 9, pp. 2031-2034, Sep. 2015.

[4] H. Choi, S. Shim, Y. Jeong, J. Lim, and C. D. Kim, "A compact DGS load-network for highly efficient class-E power amplifier," *Proceeding of European Microwave Conference*, pp. 492-495, Sep. 2009.

[5] Y. S. Lee and Y. H. Jeong, "A high-efficiency class-E GaN HEMT power amplifier for WCDMA applications," *IEEE Microwave Wireless Component Letter*, vol. 17, no. 8, pp. 622-625, Aug. 2007.

[6] A. J. Wilkinson and J. A. Everard, "Transmission-line load-network topology for class-E power amplifiers," *IEEE Transection Microwave Theory Techniques*, vol. 49, no. 6, pp. 1202-1210, Jun. 2001.

[7] A. Inoue, A. Ohta, S. Goto, T. Ishikawa, and Y. Matsuda, "The efficiency of class-F and inverse class-F amplifiers," in *IEEE MTT-S Int. Microwave Symp. Dig.*, pp. 1947–1950, Jun. 2004.

[8] Y. Jeong, G. Chaudhary, and J. Lim, "A dual band high efficiency class-F GaN power amplifier using a novel harmonic-rejection load network," *IEICE Transactions on Electronics*, vol. E95-C, no. 11, pp. 1783-1789, Nov. 2012.

[9] P. Wright, J. Lees, J. Bendikt, P. J. Tasker, and S. C Cripps, "A methodology for realizing high efficiency class-J in a linear and broadband PA," *IEEE Transection Microwave Theory Techniques*, vol. 57, no. 12, pp. 3196-3204, Nov. 2009.

[10] J. Kim, J. Moon, B. Kim, and R. S. Pengelly, " A saturated PA with high efficiency," *IEEE Microwave Magazine*, vol. 10, Iss. 1, pp. 126-133, Jan. 2009.